HHS Public Access

Author manuscript

Trends Biotechnol. Author manuscript; available in PMC 2023 October 01.

In Situ Bioprinting: Intraoperative Implementation of Regenerative Medicine

Mohamadmahdi Samandari[1,*], **Azadeh Mostafavi**[2,*], **Jacob Quint**[1], **Adnan Memic**[3], **Ali Tamayol**[1,2,‡]

[1]Department of Biomedical Engineering, University of Connecticut, Farmington, CT, USA

[2]Department of Mechanical and Materials Engineering, University of Nebraska, Lincoln, Lincoln, NE, USA

[3]Center of Nanotechnology, King Abdulaziz University, Jeddah, Saudi Arabia

Abstract

Bioprinting has emerged as a strong tool for devising regenerative therapies to address unmet medical needs. However, the translation of conventional *in vitro* bioprinting approaches is partially hindered due to their challenges associated with the fabrication and implantation of irregularly-shaped scaffolds and their limited accessibility for immediate treatment by healthcare providers. An alternative strategy that has recently drawn significant attention is to directly print the bioink into the patient's body, called *in situ* bioprinting. The bioprinting strategy and the associated bioink need to be specifically designed for *in situ* bioprinting to meet the particular requirements of direct deposition *in vivo*. In this article, we will discuss the developed *in situ* bioprinting strategies, their advantages, challenges, and possible future improvements.

Keywords

Bioprinting; *in situ* printing; handheld printers; bioinks; robotic bioprinters

Bioprinting in Regenerative Medicine

In the past decade, **bioprinting** has emerged as a tool to fabricate 3D biomimetic constructs, mainly to address the increasing need for tissue and organ grafts in regenerative medicine [5]. While the number of artificial tissue grafts has increased and improved in complexity to account for biological modulation and mechanical properties for each application, they often fail to regenerate the lost tissue, specifically in critically-sized defects, and are reduced to simple tissues. Although injected biomaterials or pre-formed injectable scaffolds conform to the wound and are suitable with minimally invasive delivery, they are limited in control

‡Corresponding author: A. Tamayol, L7075 263 Farmington Ave. CT 06030, USA; atamayol@uchc.edu.
*M. Samandari and A. Mostafavi equally contributed to this work.

over their structure, cellular organization, crosslinking mechanisms, etc., which is vital for many applications. Significant progress has been made in developing 3D bioprinting technologies and **bioinks** to facilitate complex tissue regeneration. Despite the impressive level of success of *in vitro* and *in vivo* studies in this field, bioprinting has not yet been translated properly for clinical applications. For the realization of bioprinting in clinical practice, the bioprinting strategy needs to (i) be biocompatible and pro-healing to support the viability and functionality of encapsulated and surrounding cells in the remnant tissue while promoting regenerative mechanisms; (ii) offer sufficient resolution to control the spatial distribution of different scaffolding materials, biological factors, and cells over clinically and biologically relevant dimensions; (iii) enable the reliable fabrication and implantation of the bioprinted construct into the complex defect site; (iv) be immediately accessible and easily applicable for healthcare providers; and (v) be customizable to the immunological and morphological requirements of each patient [7, 8]. While the first two above-mentioned requirements are mostly addressed in recent publications [9, 10], other requirements are yet to be met with conventional bioprinting strategies, limiting the clinical application of bioprinting for regenerative medicine [11].

Tissue defects resulting from diseases or traumatic incidents typically have irregular morphology. Therefore, the structures printed on the flat surfaces using traditional bioprinters cannot easily conform to the curved surfaces of the complex defect, specifically after *in vitro* culture which may cause degradation and deformation of the construct [12, 13]. Additionally, implantation of bioprinted constructs is challenging since they typically require secondary fixation modalities. Hydrogels, the preferred primary biomaterials for bioprinting [14–16], are difficult to suture or staple and, once fabricated, do not adhere properly to the host tissue unless chemically modified [12, 17]. Chemical modification and the use of tissue adhesives can significantly alternate the regeneration outcome. Non-adhered implants can further reduce the chance of tissue integration as a result of dislocation due to body movement after the surgery [12, 18]. Another limitation of conventional 3D bioprinters is their slow response to urgent clinical needs and the requirement of engineering expertise and infrastructure [20, 21]. For example, in the case of a traumatic injury, it takes several hours to capture 3D images from the injury site and reconstruct the computer-aided design (CAD) model to be used by current bioprinters. The printing process alone takes significant time and requires highly specialized facilities and skills. Thus, by the time that the construct is ready, a second surgery may be needed delaying patient care, potentially diminishing the regenerative properties of the remnant tissue. Therefore, there is a need for a new paradigm in the utilization of 3D bioprinters in regenerative medicine.

In situ printing: an emerging strategy for clinical translation of bioprinting

An alternative trend that recently has gained traction is to move from "*in vitro* bioprinting and subsequent implantation" toward direct printing of the bioink inside the defect, usually called "***in situ* bioprinting**", "*in vivo* bioprinting", or "intra-operative bioprinting" [17]. *In situ* bioprinting tries to realize the clinical application of bioprinting by resolving the limitations of the conventional approaches. Using an *in situ* bioprinting approach, a surgical team can immediately apply the treatment and control the procedure in real-time. Therefore, the treatment is not delayed, and at the procedure time, the surgeon is not surprised by

changes that can happen in the defect microenvironment over time due to the dynamic nature of wounds or from surgical resection and debridement. Therefore, the implanted scaffold accurately matches the defect geometry. Furthermore, the adhesion of the scaffold to the remnant tissue is enhanced through *in situ* crosslinking, improving the tissue-scaffold integration [12]. Finally, the body, implemented as a natural bioreactor, is far superior to *in vitro* culture conditions for tissue regeneration and reduces the chances of contamination [17].

In the past few years, several examples of *in situ* bioprinting strategies have been reported [13, 17, 20]. Recent research activities have focused on developing **automated *in situ* bioprinters** or **handheld printers**. While promising, *in situ* bioprinting is an emerging field that requires materials and technologies with different characteristics than conventional bioprinting. Therefore, new investigations are needed to adapt traditional bioinks and bioprinting methods to this approach. In this manuscript, we initially review various *in situ* printing methodologies and the developed tools for such applications. We will then focus on the required bioink properties for *in situ* printing and successful examples applied for the regeneration of different tissue defects. Furthermore, we will discuss the limitations of these technologies and their benefits over conventional 3D bioprinting. We will also discuss the challenges in the field and potential opportunities and applications of these technologies.

Strategies for implementing *in situ* bioprinting

Bioprinting tools used for the formation of scaffolds directly inside the patient's body can be divided into two major categories: (i) automated systems, in which the printing rate and location are controlled by computer-aided manufacturing tools, and (ii) handheld devices, in which the device controls the printing rate and printing location is controlled manually. In this section, we discuss these two device categories and highlight their differences, benefits, and limitations.

Automated in situ printing

Most conventional bioprinters are fully automated, which means that once the design is loaded into the software and the bioinks are stored in the printer cartridges or syringes, they automatically follow a G-code to fabricate a 3D scaffold. Using a similar strategy, the concept of *in situ* printing was introduced in 2007 by proposing robotic inkjet bioprinting for direct deposition of the bioink into calvarial defects [22]. During the past decade, the application of automatic *in situ* printing has significantly evolved, major limitations have been detected, and promising resolutions have been proposed [13, 17, 20]. The application of automatic systems for *in situ* printing has multiple advantages including (i) high printing accuracy, which is of significant importance in the regeneration of tissues where microsurgery is required (e.g. cornea, eardrum, etc.); (ii) rapid biofabrication of complex multimaterial scaffolds for the regeneration of large defects involving different tissues, for example in the case of a battlefield or accidental polytraumas; (iii) minimization of human errors; (iv) compatibility with minimally invasive internal surgery tools [23–25]; and (v) compatibility with closed-loop automatic controlling systems or artificial intelligence [6, 26, 27]. However, there are two main requirements for harnessing the complete potential of

automated *in situ* printing. First, automatic *in situ* printing requires an accurate scanning modality. In automatic *in situ* printers, a 3D scanner or imaging modality should be implemented to analyze the irregular geometry of each defect and export the data to a format readable by CAD software (Box 1). The CAD model, usually in standard tessellation language (STL) format, is then exported into computer-aided manufacturing (CAM) format, typically G-codes, dictating the printing strategy to the automatic bioprinter. Second, the automated bioprinting system should offer the required working space and necessary degrees of freedom (DOF) to print inside irregularly-shaped defects in the human body.

Upon the formation of the G-codes based on the STL file and bioprinting parameters, the bioprinter needs to be calibrated to the defect location [27] and start the printing process. Notably, the printed structure can be deviated from the defect model due to the poor printability of the bioink and non-ideal printing conditions on injured tissues such as wet, irregularly shaped, and moving surfaces. To resolve this issue, two main strategies have been proposed (Figure 1): error compensation before the main bioprinting procedure [28] and the application of adaptive bioprinting [26, 27]. In error compensation, the defect is scanned, a rapid prototype of the defect model is generated, a structure is bioprinted in the defect model, the printed structure is scanned, and a comparison with the 3D geometry is performed to detect accumulative errors. Then, a new G-code is generated to compensate for the errors with new bioprinting parameters (Figure 1Ai) [28]. The modified G-code is used for the actual bioprinting process *in vivo* (Figure 1Aii). However, this method is very slow and cannot compensate for errors that happened due to the printing conditions on actual tissues such as wet and deformable surfaces. The second strategy, adaptive bioprinting, can address this challenge through the application of closed-loop integrated scanning and *in situ* bioprinting systems (Figure 1B, C). Here, the scanning system provides feedback for the bioprinting device in real-time and accounts for any printing error. Interestingly, this strategy allows bioprinting on moving tissues, a reasonable improvement for *in situ* bioprinting strategies. This capability enables printing on essentially any moving body part such as lung and heart tissue (Figure 1B). Furthermore, while most procedures are performed under anesthesia, the body can still move as a result of breathing and twitching, which necessitates the error compensation by adaptive bioprinting (Figure 1C).

In situ bioprinting further needs to provide a large working space and required DOF for regenerative medicine applications. Most commercially available stationary bioprinters are small and incapable of hosting a human body or body parts. Therefore, researchers usually try to demonstrate the proof of concept by performing *ex vivo* printing on an animal carcass or harvested tissues [1, 3, 27, 29] or *in situ* printing on small animals such as mice [30–32]. In a recent study, researchers developed a large-scale frame-based integrated scanning and *in situ* printing system for the treatment of large porcine full-thickness wounds, capable of hosting the whole body [4]. While this system offers a large working area, it still suffers from limited DOF for filling the irregularly shaped defects with side cavities. A strategy to address the requirements for both working area and DOF is the application of robotic arms for *in situ* printing [27, 28, 33]. Robotic arms with six DOF (three translational and three rotational) and meters of working space can offer access to all corners of the defect and closely match or exceed the controllability of the human hand [27, 28]. However,

this technology is still under development and requires expertise for robot calibration and planning of the printing process.

Various bioprinting strategies have been adapted for automatic *in situ* printing for the treatment of skin wounds [4, 30], bone [28, 32, 34, 35], cartilage [27], brain [36], muscle [36, 37], and complex defects involving multiple tissues [38]. Extrusion bioprinting is the most widely implemented strategy for *in situ* bioprinting due to its ease of integration with *in situ* delivery systems; compatibility with various bioink viscosities and crosslinking approaches; and capability of fabricating large, complex, and multimaterial scaffolds [39]. Additionally, extrusion-based bioprinters can be easily integrated with minimally invasive surgical tools (Figure 2) [23, 24]. This allows the *in situ* printing of scaffolds without the need for prolonged open surgeries. Using minimally invasive internal bioprinting strategies, such as natural orifice transluminal endoscopic bioprinting (Figure 2A) [23] or laparoscopic bioprinting [24, 25], a less invasive treatment, even compared to implantation of pre-fabricated scaffolds, can be achieved. In an interesting recent investigation, researchers developed a minimally invasive internal *in situ* bioprinting strategy based on the nozzle deformation rather than the movement of the printing head (Figure 2B) [25]. A ferromagnetic soft nozzle was designed to access the internal tissues through a small incision and deform based on a programmable magnetic field for printing the desired structure. Using this approach, successful *in situ* printing on a living rat liver was reported. To enhance the scaffold-tissue adhesion in minimally invasive bioprinting, over-extrusion interlocking inside the remnant tissue has been suggested [24].

Other bioprinting strategies such as laser-assisted bioprinting (LAB) [34, 35], inkjet bioprinting [4, 22, 40], and stereolithography-based (SLA) bioprinting [29, 36, 37] have also been adapted for automatic *in situ* printing applications. Keriquel and colleagues [34] implemented LAB for deposition of mesenchymal stromal cell-laden nano-hydroxyapatite/collagen scaffolds directly inside a murine calvaria defect. They reported that the shape of the bioprinted scaffold could affect the treatment outcome. Furthermore, Albanna and colleagues [4] used *in situ* inkjet bioprinting for the treatment of large size wounds in murine and porcine models (Figure 3A). Their results demonstrated that an improved rate and quality of wound healing could be obtained by encapsulating autologous cells inside of the bioink. It is noteworthy that both LAB and inkjet bioprinting require relatively low viscosity bioinks, which limits the fidelity of the fabricated scaffold [41]. Since supporting structures cannot be easily used for *in situ* printing, their direct application for the treatment of defects with large complex geometries is challenging. Furthermore, due to the complexity of bioink delivery systems in these approaches, they cannot be easily integrated with minimally invasive internal surgery tools or be used for the treatment of deep and irregular shaped defects. To address these issues, different bioprinting strategies can be combined for *in situ* printing. Recently, Moncal and colleagues [38] reported the reconstruction of defected bone/skin composite tissues through a hybrid extrusion/inkjet *in situ* bioprinting approach (Figure 3B). An extrusion-based bioprinting was used to directly print paste-like acellular bone bioink into the bone defect, while inkjet bioprinting was applied to print different layers of skin with lower viscosity fibroblast-laden bioink. The results demonstrated around 80% skin regeneration after 10 days and approximately 50% bone reconstruction after 6 weeks.

In situ SLA bioprinting has also been developed recently [29, 36, 37]. Interestingly, through the application of photo-initiators sensitive to near-infrared (NIR) light, SLA can be adapted for minimally invasive internal bioprinting (Figure 4). The bioink is injected into the defect site, followed by its selective crosslinking using two-photon exposure [36] or digital micromirror device (DMD) projection (Figure 4A) [37]. Through scanning healthy tissue, reconstruction of the printing structure, and *in situ* SLA bioprinting, it has been shown that fine structures could be formed subcutaneously through intact skin. High cellular viability *in vitro* and proper tissue integration *in vivo* was reported [37]. Minimally invasive *in situ* SLA bioprinting was successfully implemented for the formation of complex structures inside murine skin, muscle, and brain [36]. Particularly, the researchers demonstrated the capability of this strategy to create biomimetic elongated structures out of photocrosslinkable gelatin encapsulating muscle-derived stem cells to induce myogenesis (Figure 4B) [36]. While it offers promising advantages over other methods, such as less invasiveness and high resolution, minimally invasive SLA-based *in situ* bioprinting is limited to photocrosslinkable bioinks and can be affected by the depth of printing [36].

While automated *in situ* bioprinting systems offer unique advantages discussed above, we anticipate that major limitations will delay the translation of these strategies from the research environment to clinical application. The scanning, CAD/CAM processing, and calibration of these bioprinters are highly complex, require multiple expertise, induce errors comparing the actual defect and fabricated structure, and increase the time to treatment. More importantly, clinicians and surgeons prefer to have a high level of control over the procedure. As a result, despite the promising developments of robotic surgery in clinical applications, surgeons still play a significant role in controlling the robotic systems during the operation. Therefore, partially-automated or **robotic-assisted bioprinting** is the anticipated strategy for *in situ* printing in upcoming years. Significant advances could be made by incorporating printing modules with existing robotic systems used for medical solutions such as those implemented for radiation therapy [42], general surgery [43], and spinal surgery [44].

Handheld in situ printing

To enhance the translational potential of *in situ* printing, researchers have tried to avoid the implementation of sophisticated automatic bioprinters through the application of partially automated handheld printers. Handheld printers are typically able to deposit the bioink at a programmed rate, while the surgeon manually controls the printing location and relative printing speed inside the defect in a direct-write fashion. Handheld bioprinting surpasses the constraints of injectable biomaterials to control spatial deposition in form and complexity, enabling the creation of organized, multimaterial, and multicellular constructs. Handheld printers are cheaper and more portable than automatic 3D bioprinters and do not require the software or hardware infrastructure of computer-driven printing approaches (scanning, CAD/CAM, spatial control systems, etc.). The smaller profile and reduced infrastructure needed for handheld printers facilitate their sterilization and increase their portability for point of care applications, especially in remote areas that are vital to military medical care or response to natural disasters. Further, the small footprint enables the deposition of biomaterials in hard-to-access, non-planar wounds; this has led to work to optimize

biomaterial drift due to gravity on angled surfaces [45]. Handheld printers also address the challenge from pre-operative imaging of changing wound geometries due to debridement, injury progression, and differences from projected and realized surgical margins.

Several handheld *in situ* printers (Figure 5) have been developed and implemented for treatment of defects in a variety of tissues: bone [46], cartilage [47–49], dental pulp [50], skin [12, 45, 51, 52], and muscle [18, 53, 54]. Most of these handheld devices have relied on extrusion-based bioprinting of hydrogel precursors, while one attempt used a melt-spinning approach for *in situ* printing of hard polymers into non-load-bearing bone defects [46]. This is mostly due to the challenges associated with the miniaturization of other bioprinting approaches such as inkjet, SLA, and LAB [20]. The user-friendly design of the handheld printers, their controllability, and flexibility of the printing pattern enables surgeons to deposit the bioinks within cracks and on curved surfaces of the injured tissue to achieve the desired structure. Therefore, most of the handheld bioprinters are developed to deposit “filaments” of soft (Figure 5A) or hard (Figure 5B) polymers to meet the desired controllability and pattern flexibility for the treatment of defects with various morphologies. The resolution in such systems can be controlled by adjusting the nozzle diameter and printing speed [12]. However, handheld *in situ* printing may not be adequate for rapidly filling defects involving large areas. In this case, handheld printers may be redesigned for their tissue- and defect-specific applications. For example, the Günther group developed handheld extrusion-based bioprinters [45, 52] for the treatment of large planar defects, particularly for burn wound healing (Figure 5C). They used a planar, multimaterial nozzle geometry that can co-deposit various hydrogels and their crosslinking agent onto clinically relevant-sized skin defects.

While handheld *in situ* printing is relatively new, its high translational potential to clinical applications enabled its fast progression toward tissue regeneration in different animal models with demonstrated improved healing and functional recovery (Table 1). Recently, Tamayol’s group developed a partially automated handheld printer with an integrated photocrosslinking mechanism and applied it for the treatment of porcine full-thickness skin wounds [12] and murine volumetric muscle loss models [18, 53] (Figure 6). Using GelMA bioinks supplemented with vascular endothelial growth factor (VEGF), Nuutila and colleagues [12] demonstrated that *in situ* printing significantly improves the quality of wound healing in terms of a lower wound contraction and a higher number of Rete Ridges (Figure 6A). The group has further progressed toward functional recovery of muscle tissues [18, 53]. Quint and colleagues [53] used the custom handheld printer to extrude filaments of a nano-engineered Muscle Ink to control the release of VEGF into a murine volumetric muscle loss (VML) injury model and demonstrated partial functional recovery after 8 weeks (Figure 6B). While the strategy demonstrated a high level of functional recovery, the results showed limited cellular infiltration into the *in vivo* printed bulk GelMA-based scaffold. To overcome the challenge of limited tissue ingrowth within bulk GelMA scaffolds, Mostafavi and colleagues [18] developed a porous foam-like GelMA bioink using a simple stirring emulsification technique to be printed directly inside VML injuries (Figure 6C). Interestingly, they demonstrated increased muscle volume, reduced fibrosis, enhanced myogenesis, and elevated innervation, as well as recovered *in situ* twitch strength and *in situ* tetanus strength, without the use of exogenous cells or growth factors.

The major challenges with the handheld printers are their lower resolution and lack of controlled spatial control. These limitations bound the level of complexity that handheld printers can recapitulate. Slowly, these challenges are being addressed to improve their usability. For example, the planar printers shown in Figure 5C use a rotating silicone wheel that controls the relative travel of the microfluidic nozzle; the hybrid approach still gives directional flexibility while maintaining uniform geometries of deposited filaments [45]. While the challenge of low resolution can be combatted by modulation of nozzle geometry and design, the handheld printing strategy is still highly skill-dependent involving human operation errors, and standardization of the surgical procedure can be challenging. The use of robotic-assistive devices to minimize noise and unwanted hand movements during the surgery can further improve their feasibility of use. Furthermore, current handheld bioprinting approaches fail to address the needs for large-scale composite tissue defects. As the technologies for all *in situ* printing technologies advance, it is expected that the level of complexity will be matched to the desired therapy and will form a continuum of care options, striking a balance between complexity and ease of use. The most economical solution for each surgical intervention, ranging from injectable biomaterials for simple defects to handheld *in situ* bioprinting for the recapitulation of structure to fully autonomous systems to precisely reconstruct complex hierarchical tissues, should be identified and optimized guided by market drivers.

Bioink requirements for *in situ* printing

Biomaterials used in regenerative medicine have general requirements including biocompatibility, biodegradability, biomimetic mechanical properties for enhanced tissue integration, and proper physiochemical cues to support cell binding, infiltration, proliferation, scaffold remodeling, and tissue maturation [14, 55]. Additionally, the biomaterials need to have good printability in their precursor form to be used as bioinks for bioprinting [39, 56]. The printability of a bioink is mainly determined by its rheological properties and gelation kinetics, based on the selected bioprinting approach and the required resolution. Therefore, the bioink and its properties need to be designed based on the bioprinting approach, the target tissue, and the encapsulated cells [39, 56]. *In situ* bioprinting strategies necessitate additional requirements to account for its unique printing environment beyond those needed for *in vitro* bioprinting (Box 2).

Various bioinks used for *in situ* bioprinting are listed in Table 1. While physical, biological, and chemical characteristics of the scaffold can be tailored by the addition of micro and nanomaterials, engraftment of functional moieties to the polymer backbone, or supplementation of synthetic materials [7, 57], natural hydrogels are preferred as the primary bioink material used for *in situ* bioprinting. Photocrosslinkable gelatin (Table 1) is one of the most widely used materials for *in situ* bioprinting due to its biocompatibility, rapid crosslinking, various cell binding and degradation sites, and tunable mechanical properties [58–60]. Interestingly, it has been reported that *in situ* crosslinking of GelMA can establish a strong adhesion to different tissues due to physical interlocking, covalent bonding from the generation of free radicals during photocrosslinking, and hydrogen bonding between free hydroxyl groups in the hydrogel structure and tissue [12, 61, 62]. This is an important aspect in the successful application of *in situ* bioprinting. Tissue

adhesion can improve implantation of engineered scaffolds and final tissue integration since it prevents their dislocation post-surgery. However, this is a major challenge for *in vitro* printed hydrogel-based scaffolds, which are not easy to suture [54]. *In situ* crosslinking generates adhesion for most bioinks via different physiochemical mechanisms, while physical interlocking can be considered as the mutual mechanism of adhesion when *in situ* bioprinting is implemented.

Collagen and fibrinogen are other primary bioink materials commonly used for *in situ* printing (Table 1). While these materials excellently mimic the *in vivo* extracellular matrix (ECM) upon crosslinking, their limited printability and slow crosslinking are not preferred for *in situ* printing of complex structures. Hyaluronic acid (HA) is another natural hydrogel widely used for *in situ* bioprinting. HA provides an ECM-like microenvironment, while its photocrosslinkable derivatives such as hyaluronic acid methacrylate (HAMA) offer rapid and easy crosslinking for *in situ* printing.

Concluding Remarks and Future Perspectives

As the area of bioprinting matures and becomes ready for clinical application, the challenges and limitations of bioprinting strategies including the slow response to traumatic events, the lack of suturability of hydrogels and their limited adhesiveness, and the need for real-time controllability and flexibility of the process during the surgery have become more prominent. One strategy that has the potential to address these challenges is to directly print scaffolding materials into the patient's body. Therefore, researchers have retrofitted conventional automated printers to be able to print directly inside the defect site. Alternatively, handheld printers were developed to deposit the bioink at a programmable rate and a location controlled by the surgeon. Both the automatic and handheld printing strategies have benefits and limitations, which need to be addressed in the future (Outstanding Questions).

While automated systems have higher accuracy, offer the potential of multimaterial *in situ* printing for the treatment of large composite defects, and are compatible with minimally invasive surgeries, they still suffer from complex equipment and limited intelligence. Current strategies usually rely on time-consuming independent steps including scanning, 3D defect model reconstruction, rectifying model imperfections, generation of G-codes based on the specific bioprinting strategy, optimization of the printing path, calibration of the bioprinter with the defect location, and finally bioprinting. Integrated systems capable of accomplishing such processes with minimal human interference are yet to be established. Artificial intelligence can be used to perform, manage, and link these processes, preferably in a closed-loop manner with the aid of different sensing modules, so the errors generated during the *in situ* printing process can be compensated and their accumulation can be prevented [8]. However, there is still a large gap between the realization of such intelligent systems and the current *in situ* bioprinters.

An existing alternative for automated *in situ* bioprinting is the application of handheld bioprinters, which are much closer to clinical translation compared to automated systems. These semi-automated devices are easy to use and do not require sophisticated facilities

and extensive expertise to operate. However, the clinical application of handheld printers should be used for defects where control over form is needed and injectable biomaterials alone do not suffice. While handheld bioprinting is empowered by human intelligence and flexibility without the need for sophisticated scanning, CAD/CAM systems, and sensing modalities, they currently suffer from skill dependency, incompatibility with minimally invasive internal surgeries, and limited capability of multimaterial printing. Importantly, the latter challenge can limit the application of handheld printers to create vasculature within the *in situ* printed scaffolds. Therefore, alternative strategies enhancing vascularization may be considered in handheld *in situ* bioprinting. One strategy is the incorporation of angiogenic factors in the bioink to improve the rate of scaffold vascularization by the host vascular network [12]. The incorporation of large pores in the printed structure can also accelerate cellular migration and vascularization of the scaffold. The integration of mesopores, with a size in the range of couple tens of micrometers, within the printed structures by handheld printers has already been reported [18, 51], with an enhanced vascularization potential [18]. Finally, multimaterial *in situ* bioprinting can be realized by integrating multicompartmental bioprinting strategies with the handheld printers to have microfluidic nozzles controlling the distribution of different bioinks in the printing filament [52, 58].

Another strategy to implement both human intelligence and robotic capabilities is the development of human-controlled robotic-assisted bioprinting systems. The development of such systems is envisaged for the near future. They can enable the utilization of minimally invasive tools that allow the delivery of scaffolds without open surgeries. The use of minimally invasive internal bioprinting is not well explored, and it is expected that innovations in applicators and crosslinking strategies are underway. Such systems can be further improved by virtual reality technologies to allow operation from a distance.

Another aspect for improving the *in situ* bioprinting field is the development of novel bioinks to address the specific requirements of *in situ* bioprinting [13]. To date, most efforts have been focused on the use of existing bioinks that are safe and biocompatible before and during the crosslinking process. However, most of the current bioinks are not designed specifically for *in situ* printing conditions (Box 2). The designed bioinks should be compatible with *in vivo* physiochemical conditions and may even benefit from such conditions. For example, *in vivo* thermal and chemical stimuli can be used as bioink stabilizers to enhance the fidelity of printed constructs. Bioinks can also be designed to interact with host tissues and enhance scaffold adhesion, improving integration; these features could be further harnessed by using *in situ* bioprinting as an adhesive and integrative layer to enable the delivery of scaffolds manufactured from more established, precise, and economical biofabrication methods. Furthermore, it is expected that the novel bioinks direct cellular differentiation and specific tissue regeneration and maturation. Finally, since *in situ* bioprinting is aimed to be used as a “point of care” strategy, methods for the storage of bioinks and patient-/tissue-specific cells should be developed.

Overall, *in situ* printing is an emerging area within the field of bioprinting and can address important challenges in the field. The new class of bioprinters is becoming a strong tool for intraoperative regenerative medicine and significant progress is expected in the next few years.

Acknowledgment

The financial support from the National Institutes of Health (R01-GM126831, R01-AR073822, R01-AR077132, T32-AR079114) is gratefully acknowledged.

Glossary:

Bioprinting
Bioprinting is an additive manufacturing strategy for fabrication of tissue-like constructs. In most cases, the construct is made of scaffolding materials carrying live cells, drugs, and biological factors. Depending on the additive process used in the fabrication of these tissue-like constructs, bioprinting methods can be classified into extrusion bioprinting, inkjet bioprinting, stereolithography (SLA) bioprinting, laser-assisted bioprinting (LAB), and non-conventional bioprinting approaches.

Bioink
Bioink is the material precursor loaded into the bioprinting system to form tissue-like constructs upon deposition and solidification. Natural and synthetic hydrogels are the most widely used primary bioink materials used for tissue engineering, particularly in regeneration of soft tissues. The primary bioink material can be supplemented with different cells, biological reagents, and micro/nanoparticles. Bioinks can be solidified after deposition to form 3D structures with various solidification mechanisms including physical phase change and chemical crosslinking.

***In situ* bioprinting**
The direct bioprinting inside tissue defects. *In situ* bioprinting is usually implemented in regenerative medicine by direct printing of bioink inside the patient's body. Therefore, it is also called *in situ* bioprinting or intraoperative bioprinting.

Automated *in situ* printers
Integrated systems in which the bioink deposition, printing path and relative printing location is controlled automatically by a computer. Usually, computer-aided manufacturing (CAM) of scaffolds by these systems require multiple supplements including a scanning system to capture the tissue defect morphology, a computer-aided design (CAD) software to reconstruct the 3D model of the defect from the scanning data, and a software to translate the CAD model and printing conditions into G-codes, understandable by the CAM system.

Handheld printers
Typically, handheld bioprinters are partially automated systems that only control the bioink deposition rate, while printing path and its relative location is controlled manually by the operator. Therefore, such systems do not require scanning and CAD/CAM tools or skills and the printing process usually relies on the operator inspection and human hand movements.

Robotic-assisted bioprinting
An *in situ* bioprinting strategy in which the human intelligence is integrated with computer accuracy. Similar to robotic-assisted surgery, a human controls the printing path and location, but through the application of a robotic system to minimize noise and unwanted hand movements. Therefore, instead of directly moving a handheld printer, a human-

controlled robotic system administrates the printing path and location. The inspection of the defect and printed structure can be further empowered by multiple cameras providing a more accurate view of the target region.

References

1. Cohen DL et al. (2010) Additive manufacturing for in situ repair of osteochondral defects. Biofabrication 2 (3), 035004. [PubMed: 20823507]
2. Gatenholm B et al. (2020) Collagen 2A Type B Induction after 3D Bioprinting Chondrocytes In Situ into Osteoarthritic Chondral Tibial Lesion. Cartilage, 1947603520903788
3. Li L et al. (2017) In situ repair of bone and cartilage defects using 3D scanning and 3D printing. Scientific reports 7 (1), 1–12. [PubMed: 28127051]
4. Albanna M et al. (2019) In situ bioprinting of autologous skin cells accelerates wound healing of extensive excisional full-thickness wounds. Scientific reports 9 (1), 1–15. [PubMed: 30626917]
5. Matai I et al. (2020) Progress in 3D bioprinting technology for tissue/organ regenerative engineering. Biomaterials 226, 119536. [PubMed: 31648135]
6. Zhu Z et al. (2021) 3D-printed multifunctional materials enabled by artificial-intelligence-assisted fabrication technologies. Nature Reviews Materials 6 (1), 27–47.
7. Elkhoury K et al. (2021) Biofabrication of natural hydrogels for cardiac, neural, and bone Tissue engineering Applications. Bioactive Materials 6 (11), 3904–3923. [PubMed: 33997485]
8. Gerdes S et al. (2021) Extrusion-based 3D (Bio)Printed Tissue Engineering Scaffolds: Process–Structure–Quality Relationships. ACS Biomaterials Science & Engineering 7 (10), 4694–4717. [PubMed: 34498461]
9. Kang H-W et al. (2016) A 3D bioprinting system to produce human-scale tissue constructs with structural integrity. Nature Biotechnology 34 (3), 312–319.
10. Kim JH et al. (2020) Neural cell integration into 3D bioprinted skeletal muscle constructs accelerates restoration of muscle function. Nature Communications 11 (1), 1025.
11. Murphy SV et al. (2020) Opportunities and challenges of translational 3D bioprinting. Nature Biomedical Engineering 4 (4), 370–380.
12. Nuutila K et al. (2022) In vivo printing of growth factor-eluting adhesive scaffolds improves wound healing. Bioactive Materials.
13. Agostinacchio F et al. (2021) In Situ 3D Printing: Opportunities with Silk Inks. Trends in Biotechnology 39 (7), 719–730. [PubMed: 33279280]
14. Annabi N et al. (2014) 25th anniversary article: Rational design and applications of hydrogels in regenerative medicine. Advanced materials 26 (1), 85–124. [PubMed: 24741694]
15. Unagolla JM and Jayasuriya AC (2020) Hydrogel-based 3D bioprinting: A comprehensive review on cell-laden hydrogels, bioink formulations, and future perspectives. Applied Materials Today 18, 100479. [PubMed: 32775607]
16. Samandari M et al. (2021) Controlled self-assembly of microgels in microdroplets. Sensors and Actuators B: Chemical 348, 130693.
17. Singh S et al. (2020) In situ bioprinting – Bioprinting from benchside to bedside? Acta Biomaterialia 101, 14–25. [PubMed: 31476384]
18. Mostafavi A et al. (2021) Colloidal multiscale porous adhesive (bio)inks facilitate scaffold integration. Applied Physics Reviews 8 (4), 041415. [PubMed: 34970378]
19. Zhang YS et al. (2021) 3D extrusion bioprinting. Nature Reviews Methods Primers 1 (1), 1–20.
20. Wu Y et al. (2020) Intraoperative bioprinting: repairing tissues and organs in a surgical setting. Trends in biotechnology 38 (6), 594–605. [PubMed: 32407688]
21. Ashammakhi N et al. (2019) In situ three-dimensional printing for reparative and regenerative therapy. Biomedical microdevices (2), 42. [PubMed: 30955134]
22. Campbell PG and Weiss LE (2007) Tissue engineering with the aid of inkjet printers. Expert opinion on biological therapy 7 (8), 1123–1127. [PubMed: 17696812]

23. Zhao W and Xu T (2020) Preliminary engineering for in situ in vivo bioprinting: a novel micro bioprinting platform for in situ in vivo bioprinting at a gastric wound site. Biofabrication 12 (4), 045020. [PubMed: 32784271]
24. Adib AA et al. (2020) Direct-write 3D printing and characterization of a GelMA-based biomaterial for intracorporeal tissue engineering. Biofabrication 12 (4), 045006. [PubMed: 32464607]
25. Zhou C et al. (2021) Ferromagnetic soft catheter robots for minimally invasive bioprinting. Nature communications 12 (1), 1–12.
26. Zhu Z et al. (2018) 3D Printed Functional and Biological Materials on Moving Freeform Surfaces. Advanced Materials 30 (23), 1707495.
27. Ma K et al. (2020) Application of robotic-assisted in situ 3D printing in cartilage regeneration with HAMA hydrogel: An in vivo study. Journal of advanced research 23, 123–132. [PubMed: 32099674]
28. Li L et al. (2020) Robotic in situ 3D bio-printing technology for repairing large segmental bone defects. Journal of Advanced Research.
29. Li W et al. (2021) A Smartphone-Enabled Portable Digital Light Processing 3D Printer. Advanced Materials 33 (35), 2102153.
30. Skardal A et al. (2012) Bioprinted amniotic fluid-derived stem cells accelerate healing of large skin wounds. Stem cells translational medicine 1 (11), 792–802 [PubMed: 23197691]
31. Skardal A et al. (2017) A tunable hydrogel system for long-term release of cell-secreted cytokines and bioprinted in situ wound cell delivery. Journal of Biomedical Materials Research Part B: Applied Biomaterials 105 (7), 1986–2000. [PubMed: 27351939]
32. Moncal KK et al. (2021) Controlled Co-delivery of pPDGF-B and pBMP-2 from intraoperatively bioprinted bone constructs improves the repair of calvarial defects in rats. Biomaterials, 121333. [PubMed: 34995904]
33. Fortunato GM et al. (2021) Robotic platform and path planning algorithm for in situ bioprinting. Bioprinting 22, e00139.
34. Keriquel V et al. (2017) In situ printing of mesenchymal stromal cells, by laser-assisted bioprinting, for in vivo bone regeneration applications. Scientific reports 7 (1), 1–10. [PubMed: 28127051]
35. Keriquel V et al. (2010) In vivo bioprinting for computer-and robotic-assisted medical intervention: preliminary study in mice. Biofabrication 2 (1), 014101. [PubMed: 20811116]
36. Urciuolo A et al. (2020) Intravital three-dimensional bioprinting. Nature Biomedical Engineering 4 (9), 901–915.
37. Chen Y et al. (2020) Noninvasive in vivo 3D bioprinting. Science Advances 6 (23), eaba7406. [PubMed: 32537512]
38. Moncal KK et al. (2021) Intra-Operative Bioprinting of Hard, Soft, and Hard/Soft Composite Tissues for Craniomaxillofacial Reconstruction. Advanced Functional Materials, 2010858. [PubMed: 34421475]
39. Samandari M et al. (2021) Bioinks and bioprinting strategies for skeletal muscle tissue engineering. Advanced Materials, 2105883.
40. Li X et al. (2017) Development of a robotic arm based hydrogel additive manufacturing system for in-situ printing. Applied Sciences 7 (1), 73.
41. Samandari M et al. (2021) 3D printing for soft musculoskeletal tissue engineering. Musculoskeletal Tissue Engineering, 167.
42. Romanelli P et al. (2018) Image-Guided Robotic Radiosurgery for Trigeminal Neuralgia. Neurosurgery 83 (5).
43. Martin-Del-Campo LA et al. (2018) Comparative analysis of perioperative outcomes of robotic versus open transversus abdominis release. Surg Endosc 32 (2), 840–845. [PubMed: 28733746]
44. Marcus HJ et al. (2014) Robot-assisted and fluoroscopy-guided pedicle screw placement: a systematic review. European Spine Journal 23 (2), 291–297. [PubMed: 23801017]
45. Cheng RY et al. (2020) Handheld instrument for wound-conformal delivery of skin precursor sheets improves healing in full-thickness burns. Biofabrication 12 (2), 025002. [PubMed: 32015225]

46. Mostafavi A et al. (2021) In situ printing of scaffolds for reconstruction of bone defects. Acta Biomaterialia 127, 313–326. [PubMed: 33705990]
47. O'Connell CD et al. (2016) Development of the Biopen: a handheld device for surgical printing of adipose stem cells at a chondral wound site. Biofabrication 8 (1), 015019. [PubMed: 27004561]
48. Duchi S et al. (2017) Handheld Co-Axial Bioprinting: Application to in situ surgical cartilage repair. Scientific Reports 7 (1), 5837. [PubMed: 28724980]
49. Di Bella C et al. (2018) In situ handheld three-dimensional bioprinting for cartilage regeneration. Journal of Tissue Engineering and Regenerative Medicine 12 (3), 611–621. [PubMed: 28512850]
50. Duarte Campos DF et al. (2020) Hand-held bioprinting for de novo vascular formation applicable to dental pulp regeneration. Connective Tissue Research 61 (2), 205–215. [PubMed: 31284786]
51. Ying G et al. (2020) An open-source handheld extruder loaded with pore-forming bioink for in situ wound dressing. Materials Today Bio 8, 100074.
52. Hakimi N et al. (2018) Handheld skin printer: in situ formation of planar biomaterials and tissues. Lab on a Chip 18 (10), 1440–1451. [PubMed: 29662977]
53. Quint JP et al. (2021) In Vivo Printing of Nanoenabled Scaffolds for the Treatment of Skeletal Muscle Injuries. Advanced Healthcare Materials 10 (10), 2002152.
54. Russell CS et al. (2020) In Situ Printing of Adhesive Hydrogel Scaffolds for the Treatment of Skeletal Muscle Injuries. ACS Applied Bio Materials 3 (3), 1568–1579.
55. Slaughter BV et al. (2009) Hydrogels in regenerative medicine. Advanced materials 21 (32-33), 3307–3329. [PubMed: 20882499]
56. Gungor-Ozkerim PS et al. (2018) Bioinks for 3D bioprinting: an overview. Biomaterials Science 6 (5), 915–946. [PubMed: 29492503]
57. Murphy SV and Atala A (2014) 3D bioprinting of tissues and organs. Nature Biotechnology 32 (8), 773–785.
58. Samandari M et al. (2021) Controlling cellular organization in bioprinting through designed 3D microcompartmentalization. Applied Physics Reviews 8 (2), 021404. [PubMed: 34084254]
59. Yue K et al. (2015) Synthesis, properties, and biomedical applications of gelatin methacryloyl (GelMA) hydrogels. Biomaterials 73, 254–271. [PubMed: 26414409]
60. Quint JP et al. (2022) Nanoengineered myogenic scaffolds for skeletal muscle tissue engineering. Nanoscale.
61. Assmann A et al. (2017) A highly adhesive and naturally derived sealant. Biomaterials 140, 115–127. [PubMed: 28646685]
62. Annabi N et al. (2017) Engineering a sprayable and elastic hydrogel adhesive with antimicrobial properties for wound healing. Biomaterials 139, 229–243. [PubMed: 28579065]
63. Ding H and Chang RC (2018) Simulating image-guided in situ bioprinting of a skin graft onto a phantom burn wound bed. Additive Manufacturing 22, 708–719.
64. Rauf S et al. (2021) Self-assembling tetrameric peptides allow in situ 3D bioprinting under physiological conditions. Journal of Materials Chemistry B 9 (4), 1069–1081. [PubMed: 33406193]
65. Kérourédan O et al. (2019) In situ prevascularization designed by laser-assisted bioprinting: effect on bone regeneration. Biofabrication 11 (4), 045002. [PubMed: 31151125]
66. O'Connell CD et al. (2020) Free-form co-axial bioprinting of a gelatin methacryloyl bioink by direct in situ photo-crosslinking during extrusion. Bioprinting 19, e00087.

Highlights:

- Bioprinting has emerged a strong tool for engineering of complex tissues, however, its clinical translation has proved to be challenging due to unreliable fabrication and implantation scaffolds and its limited accessibility.
- *In situ* bioprinting, the direct bioprinting inside the defect, has been introduced as an alternative strategy for translation of bioprinting from bench to bedside.
- Different automatic and handheld *in situ* bioprinting strategies have been developed to realize the *in situ* printing inside a patient's body.
- Both automated and handheld bioprinting strategies possess their own benefits and challenges, which should be addressed before their clinical application.
- The integration of human intelligence and accuracy of the robotic systems through the development of robotic-assisted bioprinting can be the future trend in the bioprinting field for regenerative application.

Box 1:

Scanning approaches for reconstruction of the defect geometry

Multiple scanning systems have been used for the detection of tissue defects for *in situ* bioprinting, including computed tomography (CT) [1, 2], magnetic resonance imaging (MRI) [2], and structured-light scanning (SLS) [2–4]. While CT and MRI enable volumetric scan and non-invasive internal imaging, the conventional CT and MRI imaging systems are bulky and expensive. They also fail to capture small features for high-resolution tissue engineering [2, 6]. On the other hand, SLS is much more accurate, while portable and affordable handheld SLS systems are already in the market [2, 6]. However, SLS only analyzes the surface features, which limits its application to external defects. Therefore, the scanning system should be selected based on the dimensions and position of the defects. At the next stage, the scanned data is translated into STL format using the designated scanner software, or third-party software. While called automated, irregular morphology of the defects usually necessitates multiple remodeling steps to minimize the errors during translation of point cloud dataset into 3D STL format [19]. The unknown morphology of the healthy tissue before the injury makes the formation of a 3D model even more challenging. In some instances, a mirrored or transposed scan of a healthy uninjured portion of the body could be referenced, but this is only valid for specific tissues such as an injured limb. However, despite the logistical challenges, a library of patient-specific scans could be stored and used as reference for future surgeries. This could be economically justified for high risk groups including military personnel.

Box 2:

Specific requirements of bioinks for *in situ* bioprinting

The properties of bioinks must be tailored to their printing process. *In situ* bioprinting requires further bioink properties compared to *in vitro* bioprinting that account for printing within or on live tissues. Some of the key considerations are:

1. The temperature of the printing bed for *in situ* bioprinting is fixed around body temperature (37 °C), which may affect thermal solidification of the bioink and ultimately the printing quality.
2. In contrast to *in vitro* bioprinting, support structures cannot always be used for *in situ* bioprinting, which necessitates the application of the bioinks that can form structures with high fidelity and structural stability.
3. While after *in vitro* bioprinting, the structure can be incubated for proper crosslinking before further manipulation, a rapid crosslinking is essential for *in situ* bioprinting due to the inevitable movements during and after an operation.
4. The bioink precursors and their crosslinking process need to be completely non-toxic and non-immunogenic for *in situ* printing since they are in direct contact with native tissue and the immune system. In contrast, the precursors and crosslinking process can be toxic (in acellular scaffolds) or immunogenic, as long as the final crosslinked product is biocompatible before implantation.
5. The wet environment and possibly bleeding in the defect microenvironment can not only affect the bioink concentration, but also the concentration of crosslinking reagents for *in situ* bioprinting. Furthermore, enzymatic and ionic crosslinking may be interfered with the presence of various enzymes and ions in the defect site. For example leading to premature crosslinking and clogging of the nozzle tip when extrusion-based bioprinting is used. Therefore, non-chemical crosslinking such as thermal crosslinking or photocrosslinking (if it does not cause secondary toxicity) is preferred for *in situ printing*.
6. Limited access to the defect should be considered not only for the selection of the bioprinting method but also for crosslinking of the bioink for *in situ* bioprinting. For example, photocrosslinking may not be feasible for the defects in cavities with limited access to light. Therefore, alternative strategies such as the use of lights with wavelengths having higher penetration or catheter-based illumination systems should be devised.

Outstanding Questions:

How to identify the location of different tissues and their interfaces after a polytraumatic injury and reconstruct that inside the patient's body?

How to connect *in situ* bioprinted constructs to host's circulatory and nervous system?

How to ensure the quality of the scaffolds that are *in situ* bioprinted and fix the defects as the constructs are being directly formed within the patient's body and in cases cannot easily be removed?

How to develop a robotic-assisted bioprinting strategy with ability to perform minimally invasive internal bioprinting?

How to develop point of care systems with imaging and printing capacity?

What are criteria needed by regulatory agencies to clear in situ automated bioprinters for clinical use?

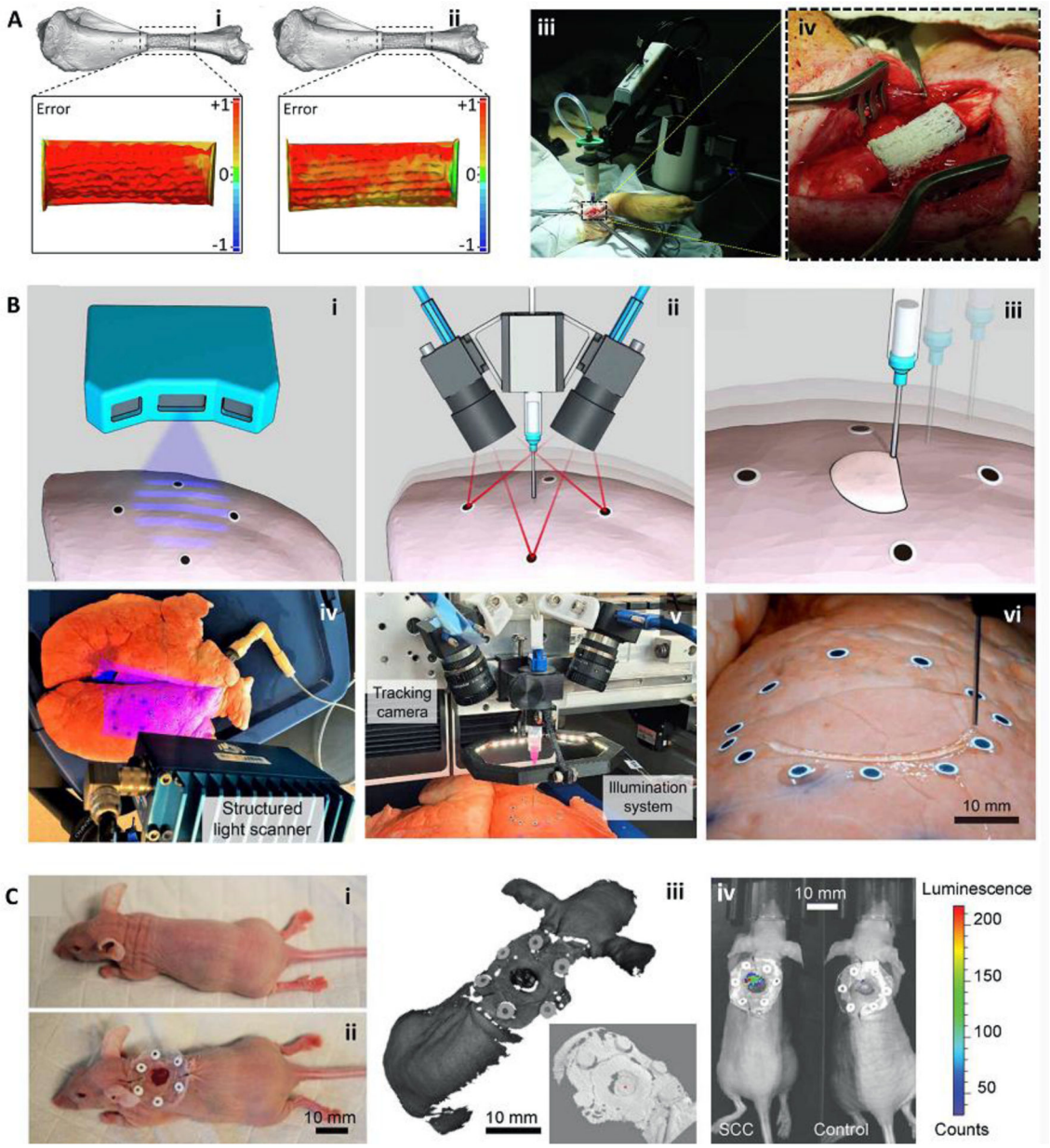

Figure 1.

Bioprinting integrated with scanning for minimizing errors during *in situ* bioprinting. (A) Error compensation before the main bioprinting procedure. Bioprinting was performed on a prototype defect model (i), the accumulative error of printing was detected with a scanner and compensated in the new printing process to reduce the error (ii). The corrected G-code was then used for *in situ* bioprinting of the bioink in a porcine long segmental bone defect (iii, iv). (B) Adaptive *in situ* printing using a closed-loop integrated scanning and printing system. The process of *in situ* printing on a breathing lung is shown schematically (i-iii), with the images of the actual setup (iv-vi). The surface of the lung was scanned (i, iv) and tracked in real-time using the fiducial guiding points (ii, v) while closed-loop feedback from the tracking module enabled printing on the moving lung (iii, vi). (C) Adaptive bioprinting

for regeneration of the skin defects in live animals. Due to the movement of the body under anesthesia, *in situ* printing strategies can be improved by using adaptive bioprinting to compensate for movements during printing. A murine model (i) was used by the creation of a full-thickness wound and placement of fiducial markers (ii). The surface was scanned (iii, zoom-in inset) and a bioink was printed inside the defect. After 4 hr, the presence of live cells was confirmed using bioluminescence imaging (iv). Adapted with permission from Elsevier [28] (A), American Association for the Advancement of Science [27] (B), and Wiley [26] (C).

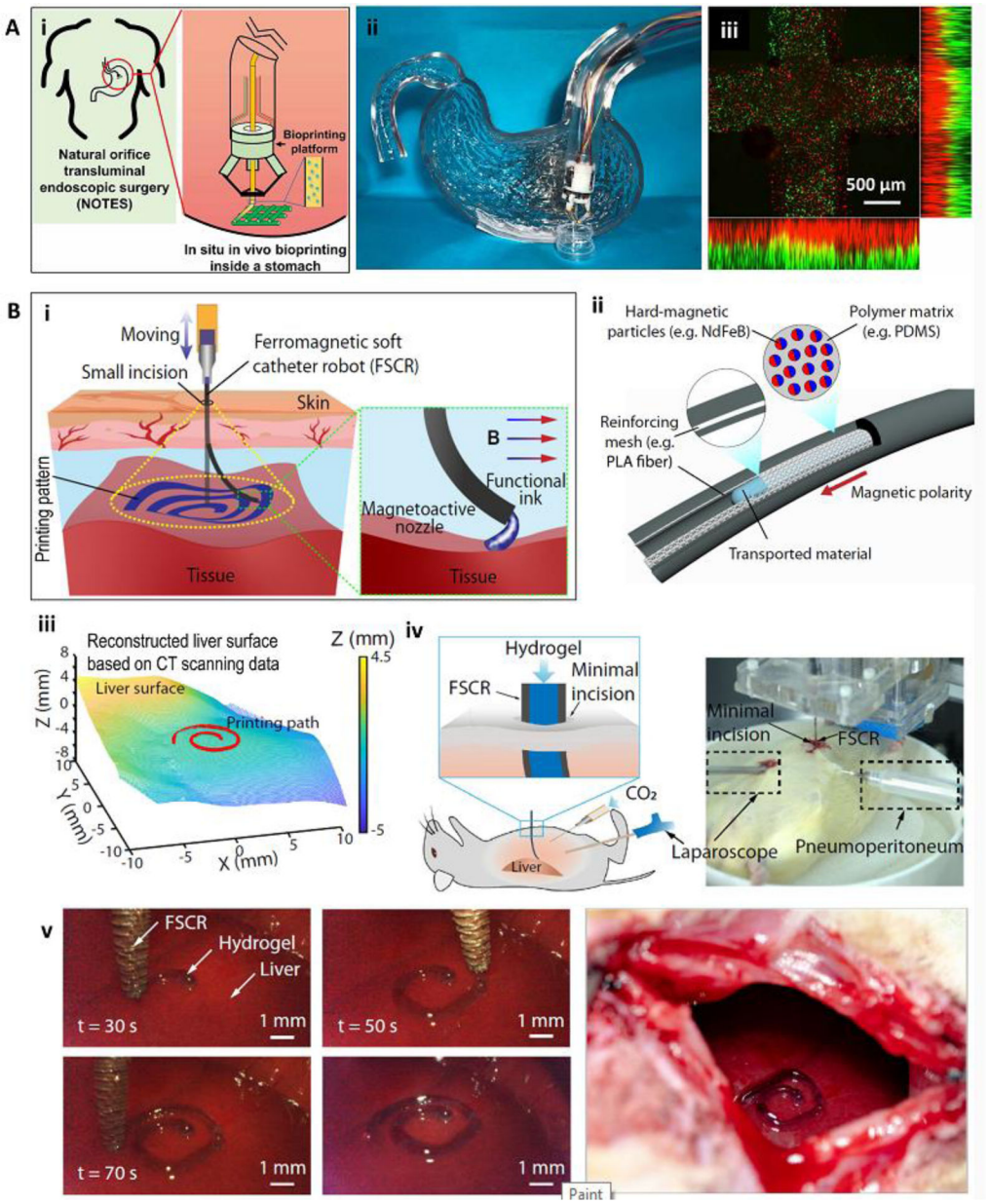

Figure 2.

Minimally invasive internal *in situ* bioprinting. (A) Natural orifice transluminal endoscopic bioprinting strategy. Schematic representation (i) and practical model (ii) of *in situ* bioprinting for treatment of gastric wall injuries. The endoscopic robot could finely print multiple layers of cell-laden bioinks with high resolution (iii). (B) Laparoscopic bioprinting using a ferromagnetic soft nozzle. The bioprinting strategy was based on the insertion of the nozzle through a small incision, and its deformation in a programmable magnetic field while extruding the bioink to form the printing structure (i). The ferromagnetic nozzle was formed from a polymeric shell embedded with magnetic particles and reinforcing fibers (ii). Minimally invasive *in situ* printing on the liver of a living rat (iii-v). The process was consisted of CT scanning to reconstruct the liver surface (iii), definition the printing path on

the upper liver surface (iii), and *in situ* printing (iv, v). The setup is shown in (iv) while a close-up view of the printing construct is shown in (v). Reproduced with permission from IOP Publishing [23] (A) and Nature Publishing Group [25] (B).

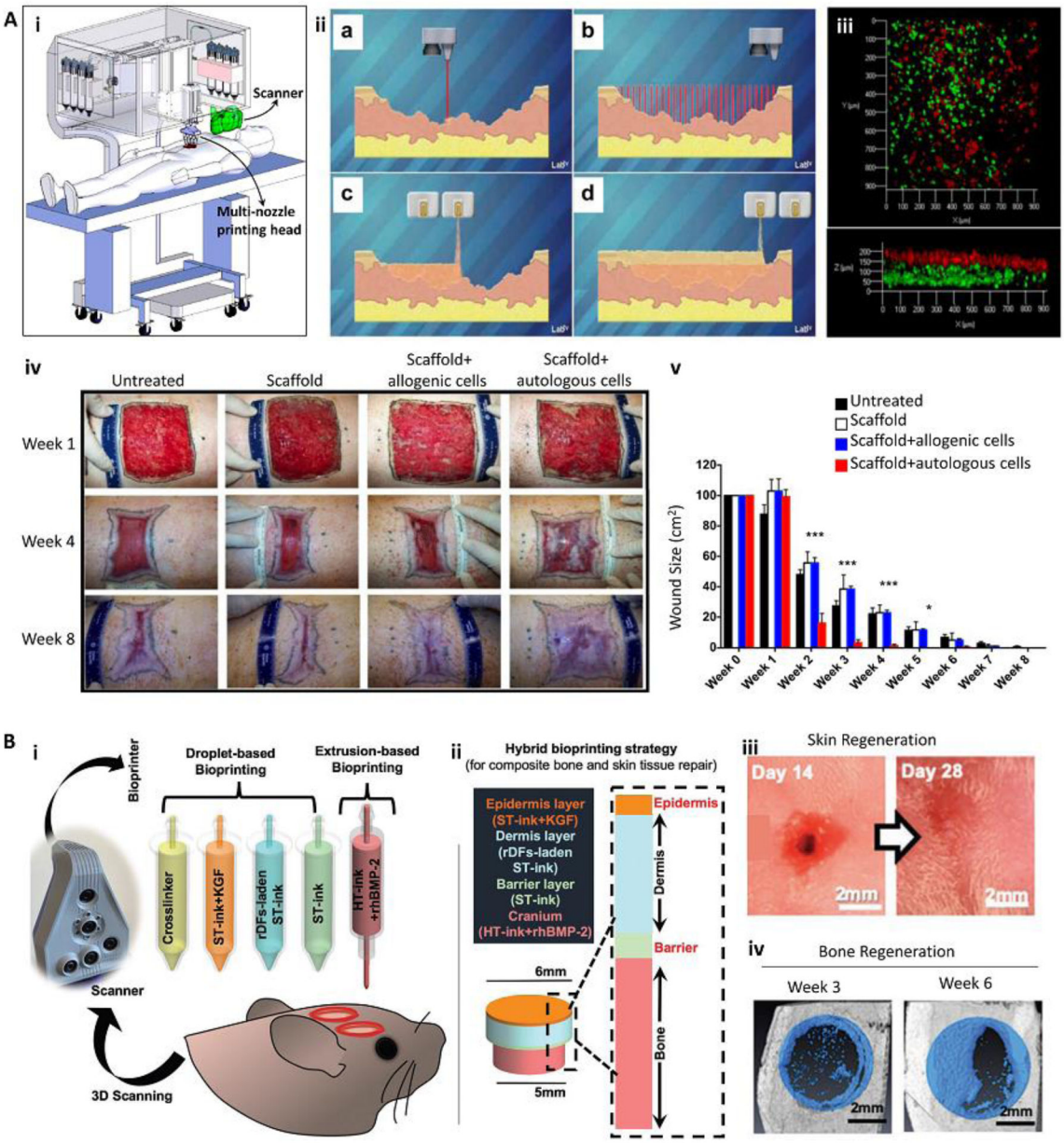

Figure 3.

In situ bioprinting for the treatment of large and complex tissue defects. (A) *In situ* bioprinting for treatment of large burn wounds. The printing approach was based on integrated scanning and multimaterial inkjet printing (i). The scanner was first used to reconstruct the defect morphology, followed by deposition of fibroblast-laden dermal and keratinocyte-laden epidermal layers (ii, iii). Fibroblasts (green) and keratinocytes (red) layers formed *in vitro* (iii). An *in situ* bioprinting on porcine burn wounds demonstrated a rapid wound closure and reduced contraction when autologous cells were encapsulated in the bioink (iv, v). (B) The treatment of complex bone/skin composite defect with a hybrid *in situ* bioprinting approach. Scanning was used to reconstruct the defect geometry, while extrusion and inkjet printing methods were implemented for *in situ* printing of high

viscosity acellular bone and low viscosity cellular skin bioinks, respectively (i, ii). Gross pictures of skin (iii) and bone (iv) tissue regeneration over 6 weeks post-surgery demonstrate major recovery of composite tissue. ST-ink: soft tissue ink consisting from collagen and fibrin; KGF: keratinocyte growth factor; rDF: rat primary dermal fibroblasts; HT-ink: hard tissue ink consisting from collagen, chitosan, nano-hydroxyapatite particles (nHAp), and β-Glycerophosphate disodium salt (β-GP); rhBMP2: recombinant human bone morphogenetic protein-2. Reproduced with permission from Nature Publishing Group [4] (A) and Wiley [38] (B).

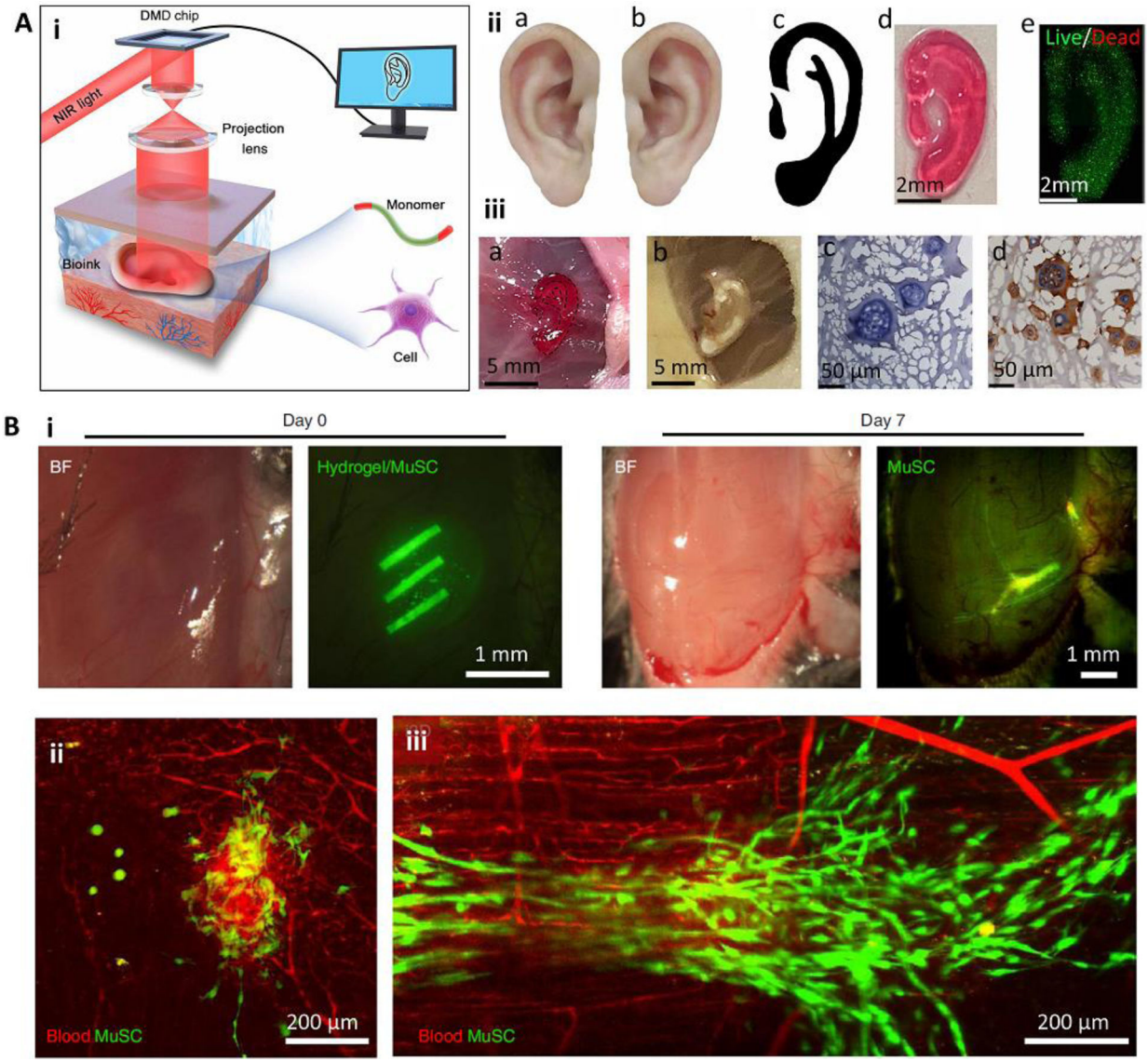

Figure 4.

Minimally invasive *in situ* SLA bioprinting. (A) The application of digital light processing for subcutaneous *in situ* bioprinting. A DMD chip was used to project NIR light through the intact skin and crosslink pre-injected cell-laden bioink (i). The *in vitro* (ii) and *in vivo* (iii) formation of an ear-like structure through intact skin. In this bioprinting strategy, the healthy tissue is scanned and mirrored to provide a representative model of the defected tissue (iia-iic). The model is then sliced and printed layer-by-layer. A fine structure with high cell viability could be achieved (iid, iie). The printed structure (iiia) was stable after 1 month (iiib), and demonstrated tissue integration by H&E staining (iiic) and immunostaining of collagen II (iiid) secreted by chondrocytes encapsulated in the printed structure. (B) Intramuscular bioprinting of scaffolds embedding muscle-derived stem cells. Elongated structures were printed to mimic the structure of native muscle (i). Results obtained after 7 days post-operation demonstrated that despite the injection of the bioink without subsequent selective crosslinking (ii), the injection of the bioink followed by selective

crosslinking for the formation of elongated structures can induce organized muscle cell (green) architectures aligned with blood vessels (red). Reproduced with permission from the American Association for the Advancement of Science [37] (A) and Nature Publishing Group [36] (B).

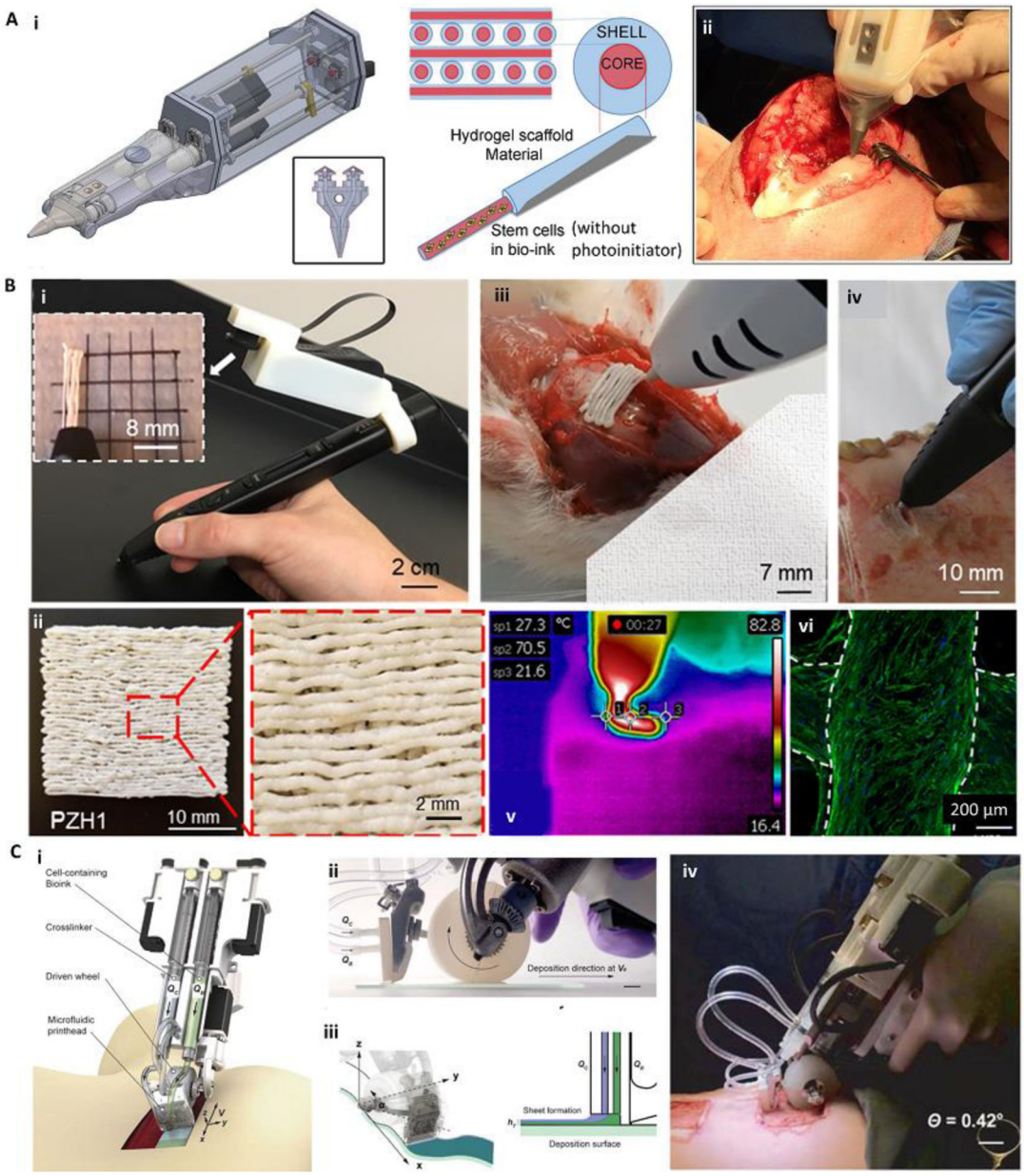

Figure 5.

Various handheld *in situ* printing strategies. (A) An extrusion-based handheld bioprinter for deposition of core-shell filaments for the treatment of osteochondral defects. The device (Bio Pen) could print a cell-laden core and a protective acellular shell (i). The Bio Pen was implemented for printing into a full-thickness osteochondral defect in the knee of a sheep (ii). (B) A melt-spinning handheld printer for treatment of bone defects. The handheld printer could be used to melt PCL-based material and deposit its filaments with a fine resolution, while a camera was integrated for better visibility (i, ii). The printer was used to fill *ex vivo* murine calvarial and porcine jaw defects (iii, iv). The temperature of the melt-extrusion filaments was shown to be lower than the threshold to induce cell death at the tissue filament interface (v). The printed scaffolds were reported to be osteoinductive after

in vitro seeding (vi). Osteopontin (green) and nuclei (blue) were immunostained on human mesenchymal stem cells differentiated into osteoblasts for 28 days. (C) An extrusion-based handheld planar printer for treatment of large burn wounds. The device could co-deposit sheets of bioink and its crosslinker to fill and conform to clinically sized and shaped skin defects (i). The planar printer had a silicone wheel to control the relative velocity of the nozzle over the defect (ii). The printer enabled two degrees of spatial control to lay down the bioink and crosslinker along non-uniform edges of a skin wound (iii). The planar printer was used for the treatment of angled porcine full-thickness burn injuries (iv). Adapted with permission from Wiley [49] (A), Elsevier [46] (B), and IOP publishing [45] (C).

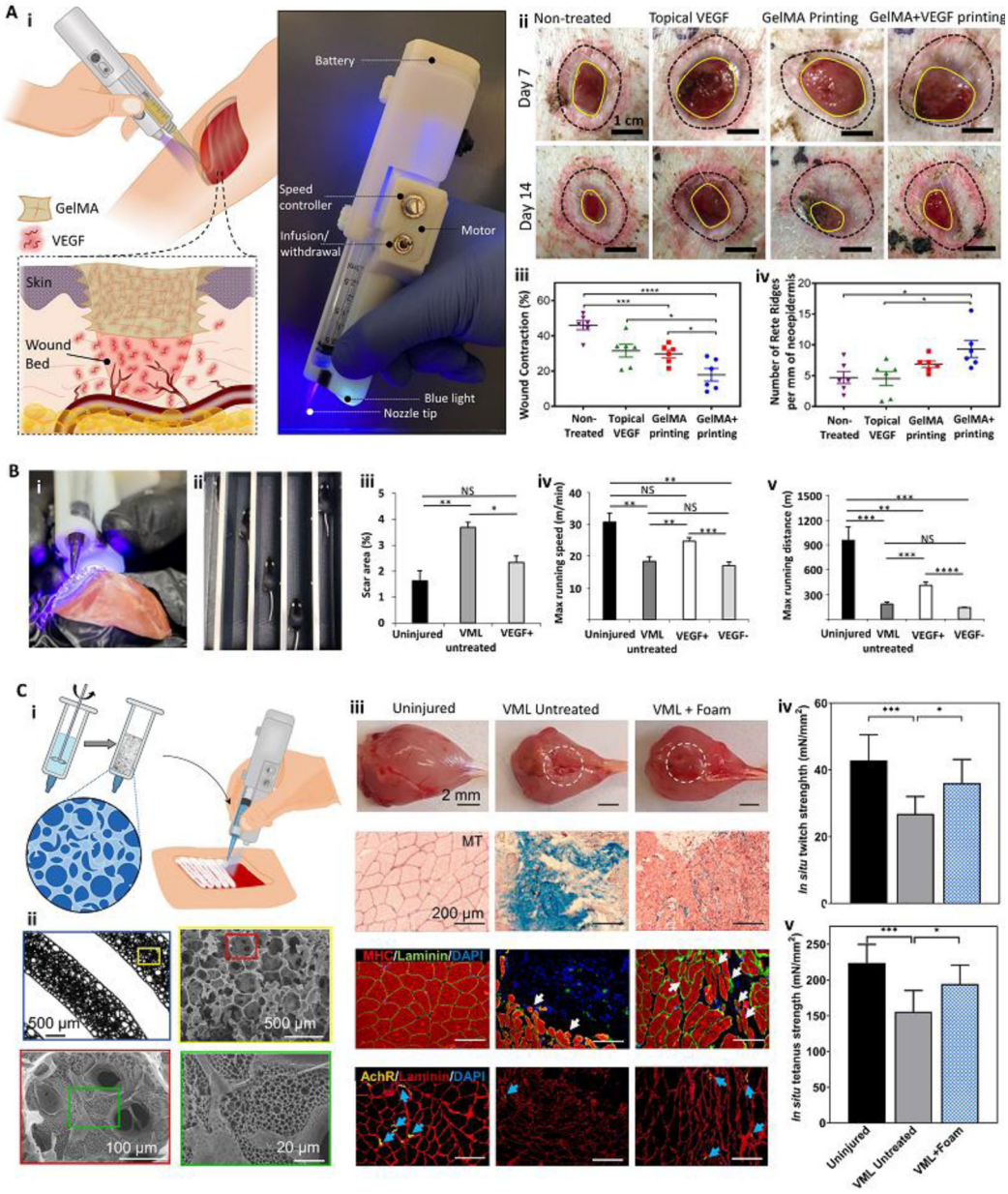

Figure 6.

Handheld *in situ* printers used *in vivo* to induce tissue regeneration and functional recovery. (A) A custom handheld printer with an integrated photocrosslinking mechanism was used for *in situ* printing of VEGF-eluting GelMA scaffolds to treat full-thickness porcine wounds (i). The handheld printed VEGF-positive scaffolds improved wound healing quality (ii). Significant reduction in wound contraction (iii) and enhancement in the number of Rete Ridges (iv) was reported. (B) The handheld printer was implemented to deposit filaments of nano-engineered Muscle Ink for skeletal muscle regeneration. The printer enabled the deposition of filaments aligned with remnant muscle fascicles (i). The effect of Muscle Ink printed within a murine VML injury model on functional recovery was evaluated using a treadmill (ii). The use of VEGF-eluting Muscle Ink reduced scar area (iii) improved the

maximum running speed (iv) and maximum running distance (v) over uninjured controls and VEGF-negative scaffolds. (C) The printer was used to deposit filaments with multiscale porosity for VML treatment. The porous bioink was developed by stirring a GelMA precursor (i). The printed foam resulted in a scaffold with hierarchical porous structures (ii). *In situ* printing of the porous bioink increased muscle volume, reduced fibrosis, improved myogenesis, and enhanced innervation after VML injury (iii). The foam scaffold induced functional recovery of the injured muscle, shown by *in situ* twitch (iv) and tetanus strength (v) results. Adapted with permission from Elsevier [12] (A), Wiley [53] (B), and AIP publishing [18] (C).

Table 1.

Bioinks and bioprinting strategies implemented for *in situ* printing.

***In situ* printing strategy**	**Printing approach**	**Scanning method**	**Bioink**	***Ex vivo/in vivo* model**	**Ref.**
Automatic (frame-based)	Extrusion	Open-loop CT	Alginate for cartilage and gelatin + demineralized bone matrix for bone	*Ex vivo*: calf chondral and osteochondral defects	[1]
Automatic (frame-based)	Extrusion	NA	Fibrinogen + Collagen	*In vivo*: murine full thickness wound model	[30]
Automatic (frame-based)	Extrusion	NA	Thiolated HA + thiolated Gelatin + polyethylene glycol diacrylate (PEGDA)	*In vivo*: murine full thickness wound model	[31]
Automatic (frame-based)	Extrusion	NA	GelMA + Laponite + methylcellulose	NA	[24]
Automatic (frame-based)	Extrusion	Closed-loop SLS	GelMA	*In vivo*: murine full thickness wound model (print on moving live animal)	[26]
Automatic (frame-based)	Extrusion	Open-loop SLS	PEGDA + Alginate	*Ex vivo*: porcine chondral and rabbit osteochondral defects	[3]
Automatic (frame-based)	Extrusion	Open-loop SLS	Alginate + Gelatin	NA	[63]
Automatic (robotic arm)	Extrusion	Open-loop SLS	GelMA + PEGDA + Alginate	*In vivo*: porcine long segmental bone defect	[28]
Automatic (robotic arm)	Extrusion	Open-loop SLS	HAMA + acrylated 4-arm PEG	*In vivo*: rabbit osteochondral defect	[27]
Automatic (frame-based)	Extrusion	Open-loop CT/MRI/SLS	Alginate + Nanocellulose	*Ex vivo*: Chondral defect	[2]
Automatic (frame-based)	Extrusion	Closed-loop SLS	Polyacrylamide + LiCl + ethylene glycol	*Ex vivo*: print on moving porcine lung	[27]
Automatic (frame-based)	Extrusion	NA	Collagen + chitosan + nano-hydroxyapatite + β-Glycerophosphate + collagen sponges + BMP2-loaded chitosan nanoparticles + PDGF	*In vivo*: murine calvarial defect	[32]
Automatic (robotic arm)	Extrusion	NA	Self-assembling peptides	NA	[64]
Automatic (endoscopic bioprinting)	Extrusion	NA	Alginate + Gelatin	NA	[23]
Automatic (laparoscopic bioprinting)	Extrusion	Open-loop SLS and CT	HA + Pluronic F127 + PEDOT:PSS + Polycarbophil	*Ex vivo*: printing on porcine hart; *In vivo*: printing on rat liver	[25]
Automatic (frame-based)	Extrusion/Inkjet	Open-loop SLS	Collagen + chitosan + nano-hydroxyapatite + β-Glycerophosphate + BMP2 for hard tissue and collagen + fibrinogen + KGF for soft tissue	*In vivo*: murine composite calvarial bone and skin defect	[38]
Automatic (robotic arm)	Inkjet	NA	PEGDA	NA	[40]
Automatic (frame-based)	Inkjet	Open-loop SLS	Fibrinogen + Collagen	*In vivo*: murine and porcine full thickness wounds	[4]
Automatic (frame-based)	Inkjet	NA	Fibrinogen	*In vivo*: murine calvaria defect	[22]
Automatic (frame-based)	SLA	NA	GelMA	*In vivo*: murine VML model	[37]
Automatic (frame-based)	SLA	NA	7-Hydroxycoumarin-3-carboxylate (HCC)-PEG or HCC-gelatin	*In vivo*: printing inside mice dermis, skeletal muscle and brain	[36]

Trends Biotechnol. Author manuscript; available in PMC 2023 October 01.

***In situ* printing strategy**	**Printing approach**	**Scanning method**	**Bioink**	***Ex vivo/in vivo* model**	**Ref.**
Automatic (frame-based)	SLA	Open-loop SLS	GelMA	*Ex vivo*: porcine muscle defect	[29]
Automatic (frame-based)	LAB	NA	Nano-hydroxyapatite solution	*In vivo*: murine calvarial defect	[35]
Automatic (frame-based)	LAB	NA	NA (cells were delivered in growth media)	*in vivo*: vascularization of murine calvarial defect	[65]
Automatic (frame-based)	LAB	NA	Collagen + nano-hydroxyapatite	*In vivo*: murine calvarial defect	[34]
Handheld	Extrusion	Not required	GelMA + polyethylene glycol	NA	[51]
Handheld	Extrusion	Not required	HAMA + GelMA	NA	[47]
Handheld	Extrusion	Not required	GelMA + gelatin + HA	NA	[66]
Handheld	Extrusion	Not required	GelMA + HAMA	NA	[48]
Handheld	Extrusion	Not required	GelMA + HAMA	*In vivo*: full thickness sheep chondral defect	[49]
Handheld	Extrusion	Not required	Collagen; Agarose + collagen; fibrinogen	*Ex vivo*: co-culture within bovine teeth	[50]
Handheld	Extrusion	Not required	GelMA	*In vivo*: murine VML injury	[54]
Handheld	Extrusion	Not required	GelMA + VEGF	*In vivo*: porcine full thickness skin wounds	[12]
Handheld	Extrusion	Not required	GelMA + Laponite + VEGF	*Ex vivo*: murine VML injury; *in vivo*: murine VML injury	[53]
Handheld	Extrusion	Not required	GelMA + PVA	*In vivo*: murine subcutaneous implantation and VML injury	[46]
Handheld	Extrusion	Not required	PCL + hydroxyapatite + ZnO	*Ex vivo*: porcine jaw bone and rat calvarial defect; *In vivo*: murine subcutaneous implantation	
Handheld	Extrusion	Not required	Fibrinogen + HA	*In vivo*: porcine full-thickness burn injury	[45]
Handheld	Extrusion	Not required	Alginate + collagen; fibrinogen + HA + collagen	*In vivo*: porcine full-thickness skin injury	[52]